IEEE Access
Multidisciplinary | Rapid Review | Open Access Journal

Received September 28, 2019, accepted October 24, 2019, date of publication October 29, 2019, date of current version November 8, 2019.

Digital Object Identifier 10.1109/ACCESS.2019.2950064

Research on Power-Balance Control Strategy of CHB Multilevel Inverter Based on TPWM

MANYUAN YE, WEI REN, LE CHEN, QIWEN WEI, GUIZHI SONG, AND SONG LI
College of Electrical and Automation Engineering, East China Jiaotong University, Nanchang 330013, China

Corresponding author: Manyuan Ye (yemanyuan1@163.com)

This work was supported in part by the National Natural Science Foundation of China under Grant 51767007, in part by the Jiangxi Provincial Industrial Science and Technology Support Project under Grant 20192BBEL50011, in part by the Jiangxi Natural Science Foundation Project under Grant 20192BAB206036, and in part by the Natural Science Foundation of Jiangxi Provincial Department of Education under Grant GJJ180306 and Grant GJJ160528.

ABSTRACT Against to the problems of low utilization rate of DC-side voltage of Cascaded H-bridge (CHB) multi-level inverter Carrier Disposition (CD) modulation strategy and unbalanced output power of each cascaded H-bridge units, a power balanced based In-Phase Disposition Trapezoidal Pulse Width Modulation (IPD-TPWM) strategy is proposed in this article. By selecting an appropriate trapezoidal wave triangulation rate δ, the modulation strategy can greatly increase the amplitude of the CHB inverter output voltage fundamental wave while ensuring the waveform quality of output phase voltage, and realize the power-balance of H-bridge units within a full modulation ratio range by changing the arrangement of triangular carriers in the vertical direction while using the carrier segment in the half carrier period of the IPD-TPWM strategy as the basic unit. Therefore, it has solved the problem of low utilization rate of DC-side voltage and unbalanced output power of each unit. At the same time, the Total Harmonic Distortion (THD) of output line voltage of the modulation strategy is lower than that of IPD-SPWM strategy in the whole modulation degree, which effectively improves the quality waveform of the output line voltage, and can be conveniently used in N-level CHB inverters. Moreover, the working stress of all the unit switching tubes is the same, the heat dissipation distribution is uniform, the switching loss is effectively reduced, and the service life and system reliability are improved. Finally, the Matlab/Simulink simulation model and experimental platform are established to verify the validity and practicality of the modulation strategy.

INDEX TERMS Cascaded H-bridge multilevel inverter, trapezoidal pulse width modulation, DC voltage utilization, power-balance, triangulation rate δ, total harmonic distortion.

I. INTRODUCTION

Cascaded H-Bridge (CHB) multi-level inverter is one of the most common multi-level inverter topologies, and has been widely used in medium voltage high-power inverters and AC drive industry. CHB multilevel inverters are characterized by many output voltage levels, excellent harmonic performance, high transmission power and easy modular design and manufacture [1]–[5]. The multi-carrier modulation strategy in the multi-level inverter modulation technology can be divided into two types: CD (Carrier Disposition) and CPS (Carrier Phase Shift) according to the difference of the spatial position of the triangular carrier. CD control can be divided into three types: In-Phase Disposition, Phase Opposition Disposition, and Alternative Phase Opposition Disposition. Among these modulation strategies, CPS-PWM strategy has the advantage of natural equalization of the output power of each cascaded H-bridge units [6], THD of output line voltage waveform is minimum under IPD-PWM strategy [7]. Although these modulation methods have their own advantages, in order to avoid over-modulation, the amplitude of sinusoidal modulation signal can not be greater than the triangular amplitude, which greatly limits the amplitude of the fundamental output voltage wave of the inverter, resulting in low utilization rate of DC-side voltage. The utilization ratio of DC side voltage can only reach 0.866 [8] under ideal condition, this shortcoming is especially obvious in high voltage and high power applications. In addition, for the traditional IPD-SPWM strategy, the fundamental amplitude of the output voltage and the output power of each cascaded H-bridge units are also

The associate editor coordinating the review of this manuscript and approving it for publication was Ho Ching Iu.

different due to the different switching time of each cascade unit, which results in the problem of unbalanced power distribution [9]–[11].

Against the above problems, Literature [12] has proposed a new PWM switching strategy for the Cascaded Multilevel Inverter (CMI). The strategy uses multiple trapezoidal modulation waveforms and a single triangular carrier to sample. Although this strategy can improve the output voltage amplitude, its experimental control process is more complicated, and the power-balance problem of each cascaded unit is not resolved. Literature [13] has proposed a novel SPWM pulse control method, which is suitable for a wide range of output voltages, provides a way to implement vector control for Induction-Motor (IM) when the cascaded Neutral-Point-Clamped (NPC) inverter is employed. The control technology first reconstructs the modulated wave, and replaces multiple carriers with a single carrier, effectively reducing the number of triangular carriers. At the same time, pulse decoding provides an effective pulse control method for the cascaded NPC inverters, and optimizes the performance of the control technology. Finally, the capacitor voltage and the power of each module are further balanced by pulse rotation. The control technology can achieve voltage balance of capacitors in each module and power-balance between the cascaded NPC inverters. However, in the control process of the cascaded NPC inverters, complex programmable logic device (CPLD) is needed to convert the logic relationship, which increases the complexity of the DSP programming control process. Literature [14] has proposed a power-balance control method based on the modulation wave period as the basic unit. The strategy takes a modulation wave period as the basic unit and moves the carrier strictly once after each modulation wave period. The strategy utilizes the output voltage redundancy characteristic of the cascading unit, and realizes the cyclic movement of the output voltage pulse by changing the cyclic movement of the carrier corresponding to each unit, and changes the cascading output voltage characteristic. However, as the number of cascaded H-bridge units increases, the time required to achieve power balancing is lengthened, and the strategy cannot improve DC-side voltage utilization. Based on the IPD-SPWM strategy, Literature [15] has proposed a power-balance control method of alternating changing the position for corresponding carrier of two units on the time axis. This strategy changes the characteristics of output voltage of each unit, and enables two units to achieve power balancing control in one output cycle. However, it adds additional switching losses to the inverters and does not solve the problem of low utilization rate of DC-side voltage. Literature [16] has proposed a hybrid multi-carrier PWM strategy, which can achieve output power-balance naturally between different units. When this strategy is applied to CHB Seven-level inverters, the THD of line voltage u_{AB} is higher or equal to CPS-PWM strategy at modulation index M∈[0.35,0.9].

This paper takes three-phase five-level inverters as an example, and has proposed an power-balance-based IPD-TPWM strategy against the problems of low utilization rate of DC-side voltage and unbalanced output power of each cascade unit in traditional IPD-SPWM strategy, and verified it by simulation and experiment.

II. IPD-TPWM STRATEGY

A. THREE-PHASE FIVE-LEVEL INVERTER TOPOLOGY

Fig.1 is a schematic diagram of the main circuit topology of a three-phase five-level inverter.

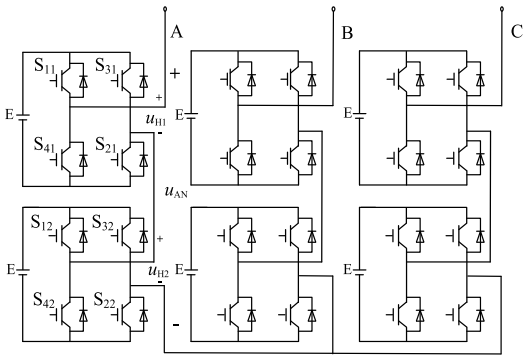

FIGURE 1. Three-phase five-level inverter main circuit topology.

u_{H1} and u_{H2} are the output voltage of two cascaded H-bridge units respectively, u_{AN} is the output phase voltage of inverter, According to the basic working principle of the CHB inverter, each H-bridge unit can output three levels (-E, 0, E), and the output phase voltage u_{AN} has five levels:±2E, ±E, 0.

B. TRAPEZOIDAL PULSE WIDTH MODULATION (T-PWM) SIGNAL

Fig.2 shows the waveform of trapezoidal modulated wave u_S, which is obtained by cutting triangular wave u_{st} through amplitude $\pm U_T$. The amplitude of triangular wave u_{st} is U_S, and the amplitudes of carrier wave and modulation wave are U_C and U_T, respectively, so the modulation ratio is M = U_T/U_C. Assuming that the amplitude ratio is $M_T = U_S/U_C$, the ratio of the trapezoidal amplitude U_T to the triangular amplitude is δ. Then the triangulation rate δ of the trapezoidal wave can be expressed as

$$\delta = \frac{U_T}{U_S} = \frac{M}{M_T} = 0 \sim 1 \tag{1}$$

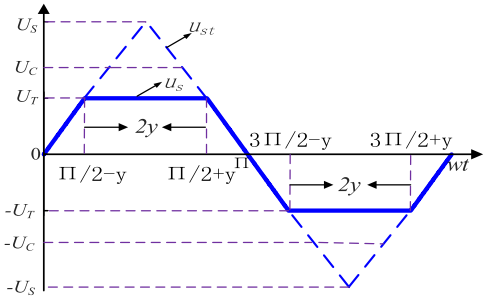

FIGURE 2. T-PWM signal waveform.

Assuming that the top edge width on the trapezoidal wave is 2y, then the relation between y and δ can be expressed as

$$y = (1-\delta)\,\pi/2 \tag{2}$$

As can be seen from Fig. 2, the trapezoidal wave is not a continuous function, so the trapezoidal wave in one cycle is divided into five regions. In each region, we can solve the angle φ of the phase intersection of the triangular carrier and the trapezoidal modulation signal.

Region 1: $0 \sim \pi/2 - y$, the slope of the trapezoidal wave u_s is $+\frac{U_S}{\pi/2}$ and the initial value is 0.

Region 2: $\pi/2 - y \sim \pi/2 + y$, $u_s = +U_T$.

Region 3: $\pi/2+y \sim 3\pi/2-y$, the slope of the trapezoidal wave u_s is $-\frac{U_S}{\pi/2}$ and the initial value is $+U_T$.

Region 4: $3\pi/2 - y \sim 3\pi/2 + y$, $u_s = -U_T$.

Region 5: $3\pi/2+y \sim 2\pi$, the slope of the trapezoidal wave u_s is $+\frac{U_S}{\pi/2}$ and the initial value is $-U_T$.

According to Literature [17], the double Fourier cardinality formula in mathematical complex form is used to express the PWM line voltage output by the inverter, as shown in Formula (3).

$$u_{AB} = \sum_{m=0}^{\infty}\sum_{n=0}^{\infty} F_{mn} y_n \exp\left[j\left(m\omega_c t + n\omega t\right)\right] \tag{3}$$

where: F_{mn} is a complex Fourier coefficient, and

$$y_n = \left\{\left[1-(-1)^n\right]\cos\left(\frac{n\pi}{6}\right) - j\left[1+(-1)^n\right]\sin\left(\frac{n\pi}{6}\right)\right\}\cdot \exp\left[j\left(\frac{n\pi}{6}\right)\right] \tag{4}$$

Then the calculated complex Fourier series F_{mn} can be expressed as:

$$\begin{aligned} F_{mn} = \left[1/\left(2\pi\right)^2\right]\Bigg(& \int_0^{(\pi/2)-y}\int_{\varphi_{a1}}^{\varphi_{b1}} e\left(x,y\right)dxdy \\ & + \int_{(\pi/2)-y}^{(\pi/2)+y}\int_{\varphi_{a2}}^{\varphi_{b2}} e\left(x,y\right)dxdy + \int_{(\pi/2)+y}^{(3\pi/2)-y}\int_{\varphi_{a3}}^{\varphi_{b3}} e\left(x,y\right)dxdy \\ & + \int_{(3\pi/2)-y}^{(3\pi/2)+y}\int_{\varphi_{a4}}^{\varphi_{b4}} e\left(x,y\right)dxdy + \int_{(3\pi/2)+y}^{2\pi}\int_{\varphi_{a5}}^{\varphi_{b5}} e\left(x,y\right)dxdy \end{aligned} \tag{5}$$

where:

$$x = \omega_c t,\ y = \omega t,\ e\left(x,y\right) = E\cdot\exp\left[-j\left(mx+ny\right)\right]$$

Substituting the calculated F_{mn} value into Equation (3) and expanding u_{AB} into a real Fourier series, the ratio of the output line voltage of the inverter to the DC side voltage is obtained as Equation (6), where:

$$\begin{aligned} u_{AB}/E = & \left(4\sqrt{3}/\pi^2\right)M_T\cos y\sin\left(\omega t+\pi/6\right) \\ & + \sum_{m=1,3\cdots}^{\infty}\sum_{n=2,4\cdots}^{\infty} A_{mn}\cos[m(\omega_c t+\pi/2) \\ & + n(\omega t+\pi/6)] \\ & + \sum_{m=2,4\cdots}^{\infty}\sum_{n=1,3\cdots}^{\infty} A_{mn}\cos[m(\omega_c t+\pi/2) \\ & + n(\omega t+\pi/6)] \\ & - \sum_{m=3,5,\cdots}^{\infty}\left[8M_T\cos\left(ny\right)/\left(n\pi\right)^2\right]\cos\left(n\pi/6\right)\cos \\ & \cdot\left[n\left(\omega t+2\pi/3\right)\right] \end{aligned} \tag{6}$$

$$A_{mn} = \begin{cases} \left[4M_T\left(M_1-M_2\right)/n\pi^2\right] & \\ \quad \sin\left(n\pi/6\right), & n \neq \pm mM_T \\ \pm\left[2\left(N_1-N_2\right)/M_T m^2 n^2\right] & \\ \quad \sin\left(mM_T\pi/6\right), & N = \pm mM_T \end{cases}$$

$$B_{mn} = \begin{cases} \left[4M_T\left(M_1+M_2\right)/n\pi^2\right] & \\ \quad \cos\left(n\pi/6\right), & n \neq \pm mM_T \\ \pm\left[2\left(N_1-N_2\right)/M_T m^2 n^2\right] & \\ \quad \cos\left(mM_T\pi/6\right), & N = \pm mM_T \end{cases}$$

$$M_1 = \sin\left[\left(n+mM_T\right)\delta\pi/2\right]/\left(n+mM_T\right),\ N_1 = mM\pi$$

$$M_2 = \sin\left[\left(n-mM_T\right)\delta\pi/2\right]/\left(n-mM_T\right),\ N_2 = \sin N_1$$

The above equations are the relationship between the output line voltage and the DC side voltage ratio under T-PWM signal. Therefore, if the phase angle ωt in Formula (6) is lagged behind $2\pi/3$ and $4\pi/3$ respectively, the expressions of voltage ratios of u_{AC} and u_{BC} to DC side can be obtained respectively.

C. SELECTION OF TRAPEZOIDAL WAVE TRIANGULATION RATE

The schematic diagram of the IPD-TPWM strategy is shown in Fig. 3. Since the choice of δ value has a great influence on the DC side voltage utilization of the CHB multilevel inverter and its harmonic characteristics, so it is necessary to conduct an in-depth analysis of the mathematical relationship between δ and the them, and select the optimal δ value based on the conclusions derived.

From Formula (6), the amplitude of the inverter output voltage fundamental and the n = 3, 5, 7, . . . harmonics can be expressed as

$$U_1 = \frac{4\sqrt{3}}{\pi^2}M_T E\cos y \tag{7}$$

$$U_n = \frac{8E_d}{\left(n\pi\right)^2}M_T E\cos\left(ny\right)\cdot\cos\frac{n\pi}{6} \tag{8}$$

From Formulas (7) and (8)

$$\frac{U_n}{U_1} = \frac{2\cos\left(ny\right)}{\sqrt{3}n^2\cos y}\cdot\cos\frac{n\pi}{6} \tag{9}$$

From Formula (2), Formula (10) can be expressed as

$$\begin{aligned} \cos\left(ny\right) &= \cos n\left(1-\delta\right)\pi/2 = \cos\left(n\pi/2 - n\delta\pi/2\right) \\ &= \sin n\delta\pi/2 \end{aligned} \tag{10}$$

$$\cos y = \cos\left(1-\delta\right)\pi/2 = \sin n\delta\pi/2 \tag{11}$$

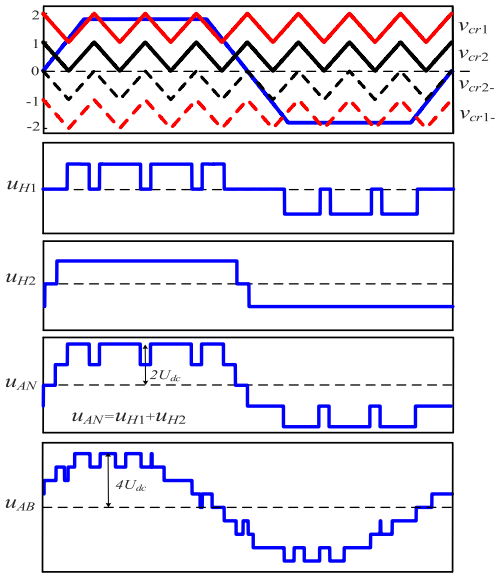

FIGURE 3. IPD-TPWM Strategy Schematic.

Substituting Formulas (10) and (11) into Formula (9)

$$\frac{U_n}{U_1} = \frac{2\sin(n\delta\pi/2)}{\sqrt{3}n^2\sin(\delta\pi/2)} \cdot \cos\frac{n\pi}{6} \tag{12}$$

From the above formulas, the total harmonic distortion rate THD of the output line voltage of the inverter can be expressed as

$$THD = \sqrt{\sum_{n=3,5}^{\infty}\left(\frac{U_n}{U_1}\right)^2} = \frac{2\sin(n\delta\pi/2)}{\sqrt{3}\,|\sin(\delta\pi/2)|} \cdot \sqrt{\sum_{n=3,5}^{\infty}\frac{2\sin(n\delta\pi/2)^2\cos(\pi n/6)^2}{n^4}} \tag{13}$$

According to the above derivation $M_T = U_S/U_C$, $\delta = U_T/U_S$, $M_T = M/\delta$ can be obtained. For TPWM inverters, when $M = 1$, the fundamental wave amplitude U_1 takes the maximum value $U_{1,M_{i=1}}$. Bring $M_T = 1/\delta$ into Formula (7) can be expressed as

$$\frac{U_{1,M_{i=1}}}{E} = \frac{4\sqrt{3}}{\pi^2\delta} \cdot \sin\delta\frac{\pi}{2} \tag{14}$$

Formulas (12), (13) and (14) respectively reflect the total harmonic distortion rate, fundamental wave amplitude and DC voltage utilization ratio of the output line voltage of TPWM inverters. It can be seen from the above formula that the harmonic content, total harmonic distortion rate and fundamental amplitude are only related to the trapezoidal wave triangulation rate δ. The relationship curves between U_n/U_1 and δ, $U_{1,M_{i=1}}$ (THD) $/E$ and δ are drawn as shown in Fig. 4 and Fig. 5 respectively.

Fig. 4 shows the relationship between U_n/U_1 and δ. Since the multiples of the third harmonic of the output line voltage cancel each other out, there is no need to analyze it. The figure contains 5th, 7th, 11th and 13th harmonics.

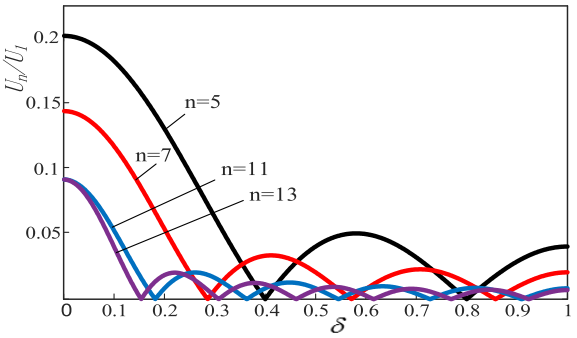

FIGURE 4. The relationship between the relative amplitude of each harmonic and the triangulation rate δ.

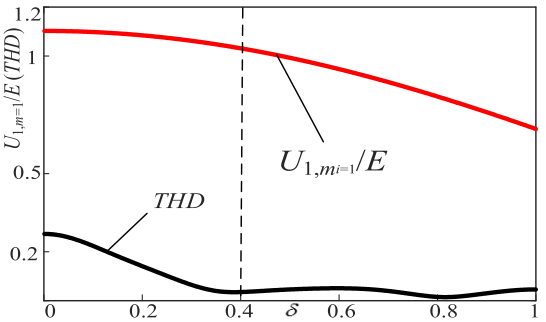

FIGURE 5. Relationship between DC voltage utilization rate and waveform distortion coefficient and triangulation rate δ.

When $\delta = 0.4$, although the 7th harmonics content is slightly higher than the 7th harmonics content at $0.3 \leq \delta \leq 1$, the 5th harmonics content is 0, and the 11th and 13th harmonic contents are also small.

As can be seen from Fig.5, when δ is small, the DC voltage utilization ratio of IPD-TPWM strategy exceeds 1, which is much larger than 0.866 of SPWM strategy. As the value of δ increases from 0 to 1, $U_{1,M_{i=1}}/E$ decreases gradually, then trapezoidal wave becomes triangular wave, and the utilization ratio of DC voltage decreases with the increase of value of δ.

As can be seen from Fig. 5, considering the fundamental amplitude of output voltage and the total harmonic distortion rate of line voltage under different δ values, the trapezoidal wave at $\delta = 0.4$ can be determined to be the best trapezoidal modulation wave.

III. POWER-BALANCE-BASED IPD-TPWM STRATEGY

A. CARRIER RECONSTRUCTION PRINCIPLE OF IPD-TPWM STRATEGY

Although the IPD-TPWM strategy can improve the problem of low utilization rate of DC-side voltage, the output voltages of each cascaded units of the CHB inverters are still not equal, and the equalization control of the output power of each unit cannot be achieved. Therefore, an power-balance-based IPD-TPWM strategy is proposed in the paper against the shortcomings of IPD-TPWM strategy. This strategy takes half carrier period of IPD-TPWM strategy as the basic unit, and changes the arrangement of the triangular carriers in the

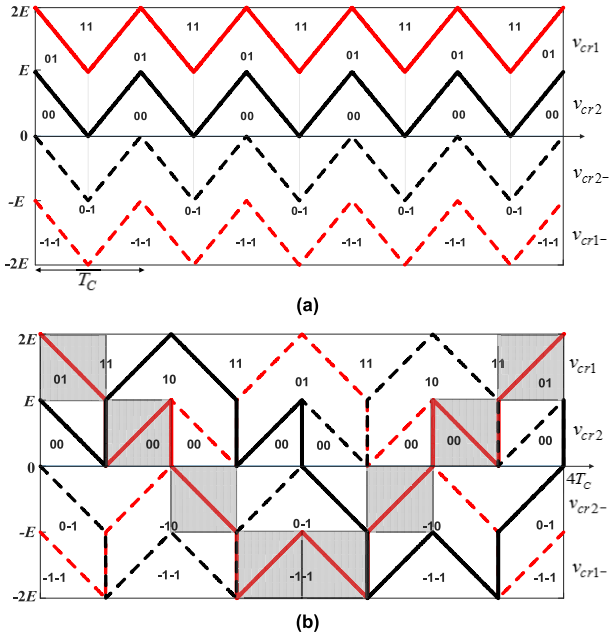

FIGURE 6. Carrier reconstruction diagram (a) Before carrier reconstruction (b) After carrier reconstruction.

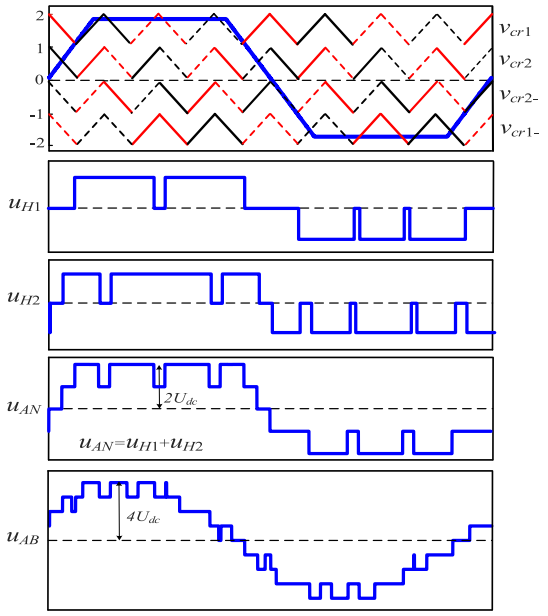

FIGURE 7. Schematic diagram of power-balance-based IPD-TPWM strategy.

vertical direction through periodic cycles, it can solve the problems of low utilization of DC-side voltage and unbalanced output power of each cascaded unit.

The schematic diagram of the strategy is shown in Fig. 6. In the carriers of IPD-TPWM strategy, the triangular carrier period is set as T_C, and the carrier segment in the half carrier period T_C /2 is taken as the basic unit. At the end of each half carrier period, the carrier segment is moved vertically once, and after 8 times of movement, a cycle is completed. At this time, the period of reconstructed carrier is $4T_C$. As shown in Fig.6(b), the carrier segments in the eight shaded regions constitute a reconstructed carrier cycle in the power-balanced IPD-TPWM strategy, and the remaining three reconstructed carriers are sequentially phase-shifted by a quarter of the reconstructed carrier cycle. Each cascading unit corresponds to a pair of reconstructed carrier signals of v_{cri} and v_{cri-} in Fig. 6(b).

Supposing S_i as a switching function of cascaded unit i ($i = 1, 2$) output level state, when $u_{Hi} = E$, $S_i = 1$; when $u_{Hi} = 0$, $S_i = 0$; and when $u_{Hi} = -E$, $S_i = -1$. Then the output voltage u_{Hi} of cascade unit i can be expressed as

$$u_{Hi} = S_i E \tag{15}$$

Then the inverter output phase voltage is expressed as

$$u_{AN} = E \sum_{i=1}^{2} S_i \tag{16}$$

The switching function of the inverter output level state is defined as S, and $S = (S_1 S_2)$. The output voltage of cascaded units remains unipolar, that is, when u_{AN} is positive, u_{Hi} can only be E or 0; when u_{AN} is negative, u_{Hi} can only be $-E$ or 0.

According to the logical relationship between the modulation wave and carrier waves, the switching function S of inverter output level state can be obtained when the modulation wave is in different regions. Fig. 6 shows the comparison of switching function S before and after carrier reconstruction. In Fig. 6(a), IPD-PWM strategy has only five switching function states: 11, 01, 00, 00-1, 0-1 and −1-1, which correspond to the output phase voltages of the inverters $2E$, E, 0, $-E$ and $-2E$, respectively. The switching function S after carrier reconstruction is shown in Fig. 6 (b). By comparison, it is found that when the output voltage u_{AN} is E or -E, power-balance-based IPD-TPWM strategy makes use of the two redundant switching function states of 10 and −10. It can be seen that although the output TPWM voltage is exchanged between the two H units, the total output voltage of the inverter has not changed.

B. IPD-TPWM STRATEGY POWER-BALANCE ANALYSIS

Fig.7 shows the modulation principle of power-balance-based IPD-TPWM strategy. Compared with the modulation principle of IPD-TPWM strategy shown in Fig. 3, it can be seen that the proposed strategy utilizes the redundant switching function states of the inverter, the output voltage characteristics of each cascaded H-bridge unit can be changed by adjusting the arrangement of carriers in vertical direction, but the output level state of the inverters can not be changed. This creates conditions for realizing power-balance control between cascaded units.

In order to illustrate the mechanism of power equalization based on the power-balance IPD-TPWM strategy, the output voltage characteristics of the cascading unit in the reconstructed carrier cycle are analyzed. Assuming that

the reconstructed carrier frequency is much larger than the sinusoidal modulated wave frequency, the sinusoidal modulated wave and the inverter output current can be considered constant values during the reconstructed carrier period.

Fig. 8 shows the cascading unit and CHB inverter output voltage conditions for the power-balanced IPD-TPWM strategy during the positive half cycle. In the figure, the CHB inverter output voltage is located in the interval [*0, E*] as an example.

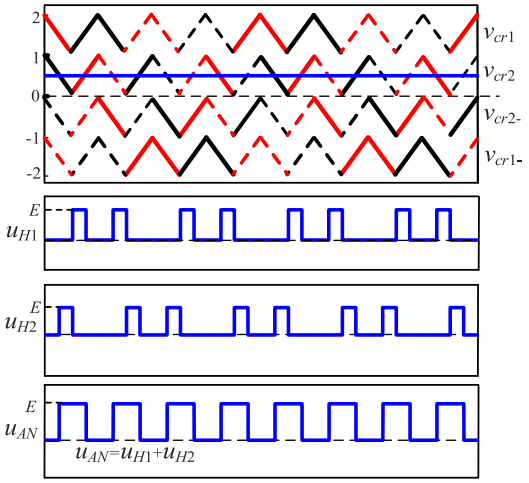

FIGURE 8. Output analysis of power-balance control method in the positive half cycle.

Assuming that the reconstructed carrier period is T_C', in the interval [*0, E*], t_{Hi+} represents the time when the cascading unit *i* outputs the voltage *E* in the reconstructed carrier period, then t_{Hi+} can be expressed as

$$\begin{cases} t_{H1+} = \dfrac{T_C'}{4} v_m \\ t_{H2+} = \dfrac{T_C'}{4} v_m \end{cases} \tag{17}$$

Then the average value of the output voltages $\overline{u}_{H1+}$ and $\overline{u}_{H2+}$ in the reconstructed carrier cycle of each cascaded unit is represented as

$$\begin{cases} \overline{u}_{H1+} = \dfrac{v_m}{4} E \\ \overline{u}_{H2+} = \dfrac{v_m}{4} E \end{cases} \tag{18}$$

Since the output current of each cascade unit is equal and constant, it can be known from the formula (18) that the average power $\overline{P}_{H1+}$ and $\overline{P}_{H2+}$ of the respective cascading units are equal in the reconstructed carrier period.

$$\overline{P}_{H1+} = \overline{P}_{H2+} \tag{19}$$

Fig. 9 shows the cascading unit and CHB inverter output voltage conditions for the power-balanced IPD-TPWM strategy during the negative half cycle. In the figure, the CHB inverter output voltage is located in the interval [*-E,0*] as an example.

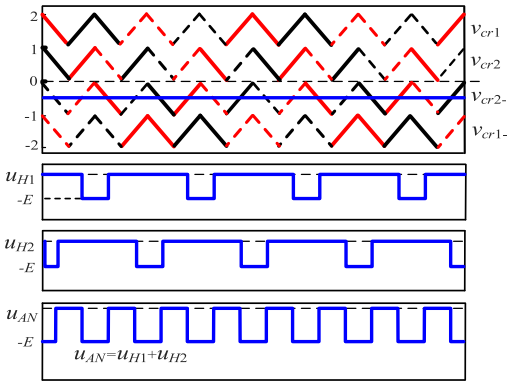

FIGURE 9. Output analysis of power-balance control method in the negative half cycle.

Assuming that in the interval [*-E, 0*], t_{Hi-} represents the time when the cascading unit *i* outputs the voltage *-E* in the reconstructed carrier period, then t_{Hi-} can be expressed as

$$\begin{cases} t_{H1-} = \dfrac{T_C'}{4} v_m \\ t_{H2-} = \dfrac{T_C'}{4} v_m \end{cases} \tag{20}$$

Then the average values of the output voltages $\overline{u}_{H1-}$ and $\overline{u}_{H2-}$ in the reconstructed carrier cycle of each cascaded unit are represented as

$$\begin{cases} \overline{u}_{H1-} = \dfrac{v_m}{4} E \\ \overline{u}_{H2-} = \dfrac{v_m}{4} E \end{cases} \tag{21}$$

It can be known from the Formula (21) that the average power $\overline{P}_{H1-}$ and $\overline{P}_{H2-}$ of the respective cascading units are equal in the reconstructed carrier period.

$$\overline{P}_{H1-} = \overline{P}_{H2-} \tag{22}$$

Therefore, on the basis of the IPD-TPWM power, the carrier is reconstructed by changing the arrangement of carriers in the vertical direction, so that the output voltages of the various units are equal in one reconstructed carrier cycle, thus ensuring that the output power average values of each cascaded unit is equal and the time required for power-balance is one reconstructed carrier period.

C. APPLICATION OF POWER-BALANCE-BASED IPD-TPWM STRATEGY IN N LEVEL CHB INVERTER

The power-balance-based IPD-TPWM strategy can not only realize the power-balance under the CHB five-level inverter, but also can be extended to the N-level CHB inverter, which can realize the power-balance control.

Fig. 10 is a schematic diagram of carrier reconstruction of a CHB seven-level inverter. Fig. 10 (a) and Fig. 10 (b) are IPD schematic diagrams of seven-level inverters before and after carrier reconstruction, respectively. By comparison, it is found that when the output voltage u_{AN} takes $2E$, E, $-E$ and $-2E$, the power-balance-based T-PWM strategy makes

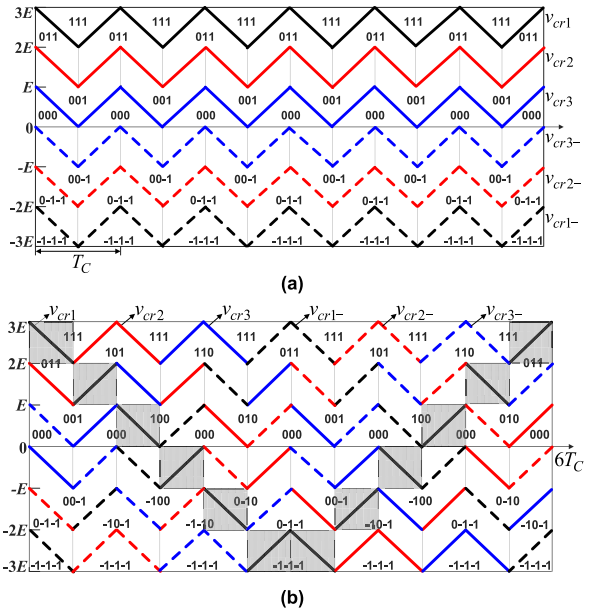

FIGURE 10. Carrier reconstruction diagram (a) Before carrier reconstruction (b) After carrier reconstruction.

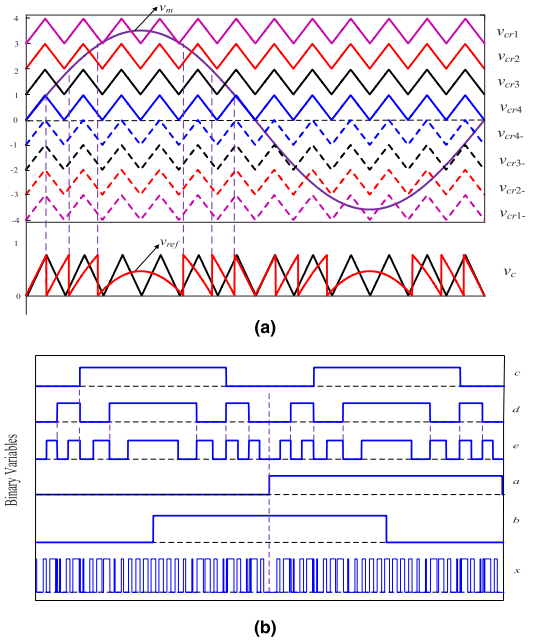

FIGURE 11. The strategy proposed in literature [13] (a) The modulation principle diagram of literature [13] (b) Principle of pulse decoding.

use of the eight redundant switching function states of 101, 110, 100, 010, −100, 0-10, −10 − 1 and −1 − 10, but does not change the output voltage u_{AN} of the inverters. The figure takes a carrier segment within half carrier period $T_C/2$ as a basic unit. At the end of each half carrier period, the carrier segment is moved vertically once, and after 12 times of movement, a cycle is completed. At this time, the period of reconstructed carrier is $6T_C$.

Similarly, the carrier segment in the half-carrier period $T_C/2$ of the CHB nine-level inverter carrier is the basic unit, and one cycle period is completed after moving 16 times, and the reconstructed carrier period becomes $8T_C$. The other N-level inverters are analogous.

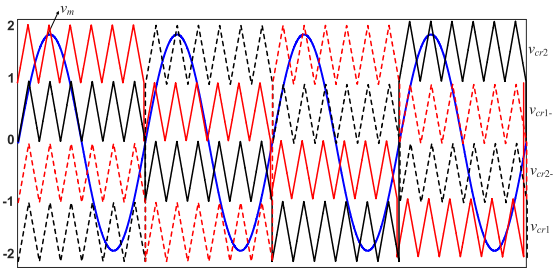

FIGURE 12. The modulation principle diagram of literature [14].

IV. OPTIMAL MODULATION STRATEGY

A. TWO COMMON POWER BALANCED STRATEGIES

Against the defects of IPD-SPWM strategy, each of Literature [13], [14] and [15] has proposed a power-balance strategy respectively. Literature [13] presents a novel SPWM pulse control method, which is suitable for a wide range of output voltages, provides a way to implement vector control for IM when the cascaded NPC inverter is employed. The modulation principle of Literature [13] is shown in Fig. 11 (a). The modulation strategy uses a single carrier to replace multiple carriers, effectively reducing the number of triangular carriers. At the same time, pulse decoding provides an effective pulse control method for cascaded NPC inverters, and optimizes the performance of the control technology, as shown in Fig. 11 (b). Finally, the capacitor voltage and the power of each module are further balanced by pulse rotation. Literature [13] applies the power-balance control method to the topology of cascaded NPC inverters. Although the capacitor voltage balance of NPC inverters and the output power-balance control of each cascade module are realized, the strategy requires complex programmable logic device (CPLD) to convert the logic relationship, which increases the difficulty of the system control. There is still a certain gap between the strategy proposed in Literature [13] and the strategy proposed in this paper, so it is not suitable for application in CHB inverter topology.

Literature [14] proposed a power equalization control method based on the modulation wave period as the basic unit. The modulation principle of Literature [14] is shown in Fig. 12. The strategy takes a modulation wave cycle as the basic unit. In the vertical direction region, the carrier is moved strictly once after each modulation wave cycle, and a carrier cycle is completed after three times of movement. At this time, the carrier cycle is four modulation wave cycles. The strategy compensates the power imbalance caused by spatial dimension through time dimension, and achieves power-balance control in two modulation wave cycles.

Based on the IPD-SPWM strategy, Literature [15] proposes a power-balance control strategy of exchanging the position for corresponding carrier of two units on the time axis. The modulation principle of Literature [15] is shown in Fig. 13.

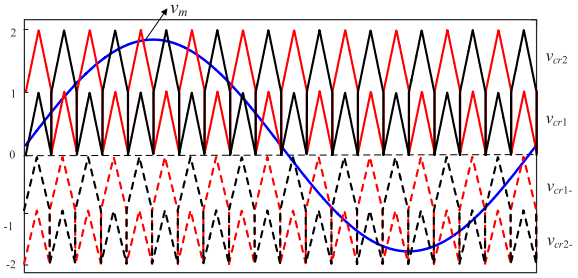

FIGURE 13. The modulation principle diagram of literature [15].

V. SIMULATION ANALYSIS

In order to verify the effectiveness of power-balance-based IPD-TPWM strategy, two commonly used power-balance strategies, IPD-TPWM strategy and power-balance-based IPD-TPWM strategy are simulated and validated respectively. In order to ensure that the inverters have the same switching frequency, the carrier frequency of the power-balance-based IPD-TPWM strategy and the commonly used power balancing strategy are set to 750 Hz and 3000 Hz, respectively. The relevant parameters of the model are shown in Table 1.

TABLE 1. Simulation parameters.

parameters	Numerical value
DC voltage E/V	50
Amplitude modulation index m_a	0.9/0.6
Fundamental frequency f_S /HZ	50
Carrier ratio m_f	60
Filter inductor L/mH	2
Load Resistance R/ Ω	10
Triangulation rate δ	0.4

The simulation waveform of power equalization control method proposed in Literature [14] is shown in Fig. 14. As can be seen from Fig. 14 (a), the switching-on time of each cascade unit is the same, the number of switches is also nearly the same, so the output voltage amplitudes are almost equal;

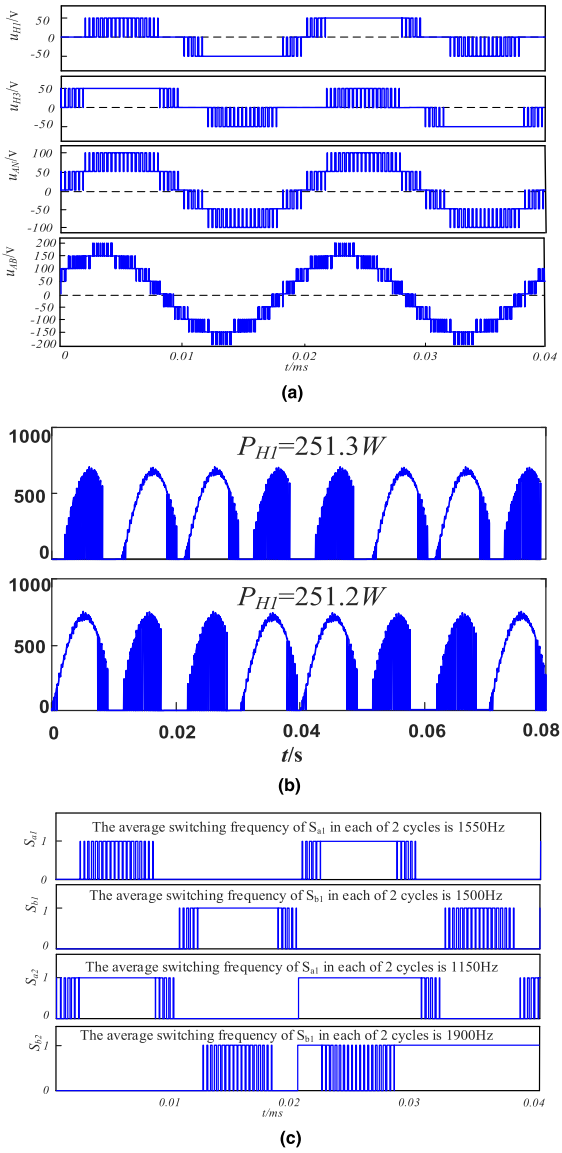

FIGURE 14. Strategy proposed in literature [14] (a) Voltage output characteristics of literature[14] (b) Output Power of each Unit (c) Driving signal of the switching tube.

As can be seen from Fig. 14 (b), this strategy compensates the power imbalance caused by spatial dimension through time dimension, and achieves power-balance control in two modulation wave cycles. As can be seen from Fig. 14 (c), when the equivalent switching frequency of the inverter is 3000Hz, the average switching frequency of all switches is different in two cycles, and the switching loss distribution is uneven. And the more cascaded H-bridge units, the longer time it takes to achieve power equalization, so this strategy is suitable for the occasion of fewer cascaded units.

The simulation waveform of power equalization control strategy proposed in Literature [17] is shown in Fig. 15. As can be seen from Fig. 15 (a), the switching-on time of each cascade unit is the same, the number of switches is also nearly the same, so the output voltage amplitudes are almost equal;

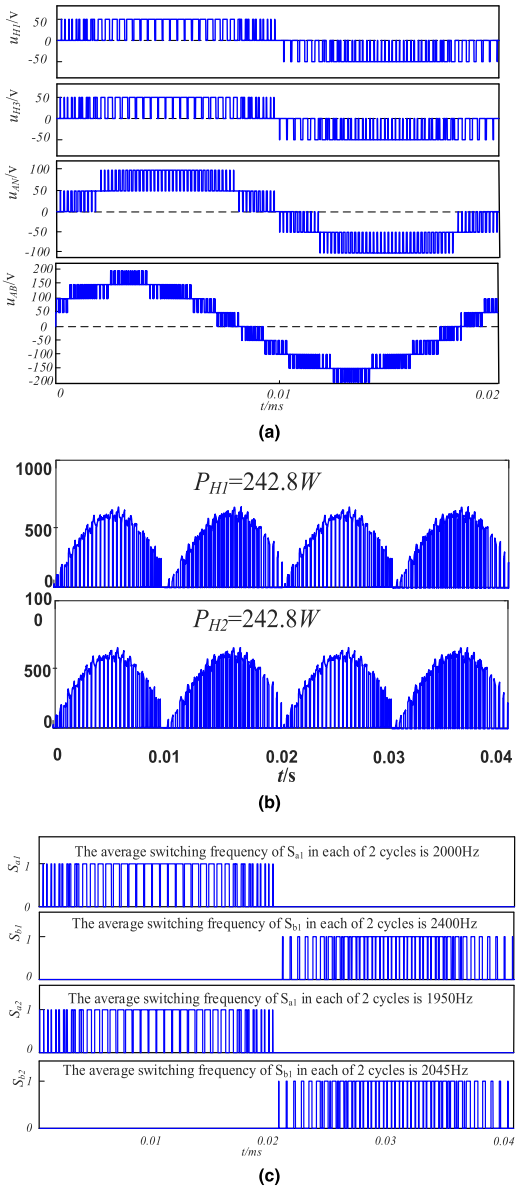

FIGURE 15. Strategy proposed in literature [15] (a) Voltage output characteristics of literature[15] (b) Output power of each Unit (c) Driving signal of the switching tube.

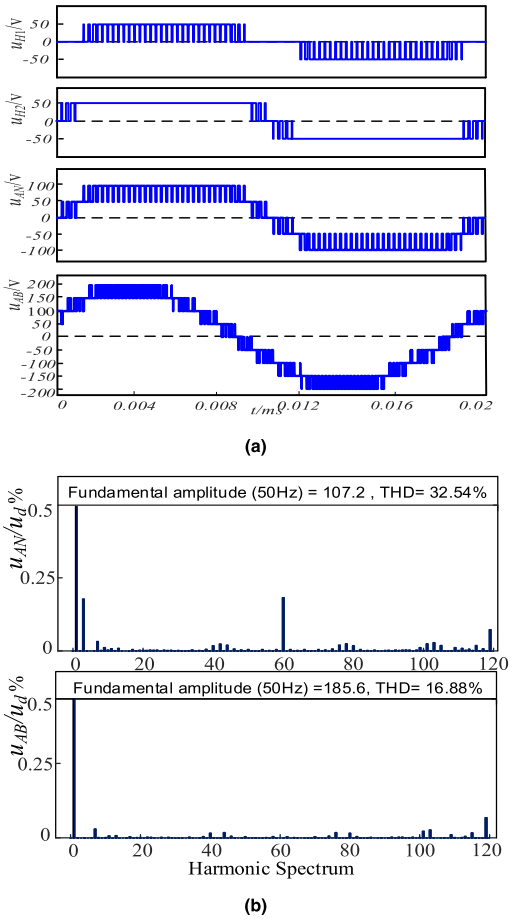

FIGURE 16. IPD-TPWM Modulation Strategy (a) with Output voltage characteristics of IPD-TPWM Strategy (b) with Harmonic spectrum analysis of output voltage.

Characteristics of output voltage of each cascaded unit can be changed through alternating changing carrier in vertical direction, and power-balance control is realized in 1 cycle, as shown in Fig. 5(b). When equivalent switching frequency of inverter is 3000Hz, driving signal of all switching tubes in 1 cycle is shown in Fig 5(c). Obviously, it can be seen from Fig.5 (c), the average switching frequency of all switching tubes in each of 1 cycles is different, so switching loss is distributed unbalanced. Moreover, compared with IPD-PWM technique, it has increased the working frequency of all switching tube in each of a cycle, and this strategy has not solved the problem of low DC voltage utilization.

Fig. 16 show the output voltage waveform and harmonic spectrum analysis of the CHB inverter under the IPD-TPWM strategy when the triangulation rate is 0.4 and the modulation ratio is 0.9.

Fig. 16 (a) shows the waveforms of the output voltage, phase voltage and line voltage of each unit under the IPD-TPWM strategy. It can be seen from the figure that the on-times of the switching tubes of the respective cascade units are inconsistent, and the number of switches is different, so the amplitudes of the output voltages are greatly different.

Fig. 16 (b) shows the spectrum analysis of the line voltage and phase voltage output waveforms of the IPD-SPWM strategy. It can be seen from the figure that the THD of u_{AN} and u_{AB} in phase A is 32.54% and 16.88%, respectively, and the THD of u_{AN} and u_{AB} in IPD-SPWM strategy in Literature [18] is 33.29% and 17.35%, respectively. The THD of u_{AN} and u_{AB} under IPD-TPWM is lower than that of the traditional IPD-SPWM, so IPD-TPWM retains the advantage of low harmonic content of output voltage in IPD-SPWM.

As can be seen from Fig. 16(b), the fundamental amplitudes of u_{AN} and u_{AB} under the IPD-TPWM strategy is 107.2V and 185.6V, respectively. In the literature [18], the fundamental amplitude of IPD-SPWM is 90V and 156V

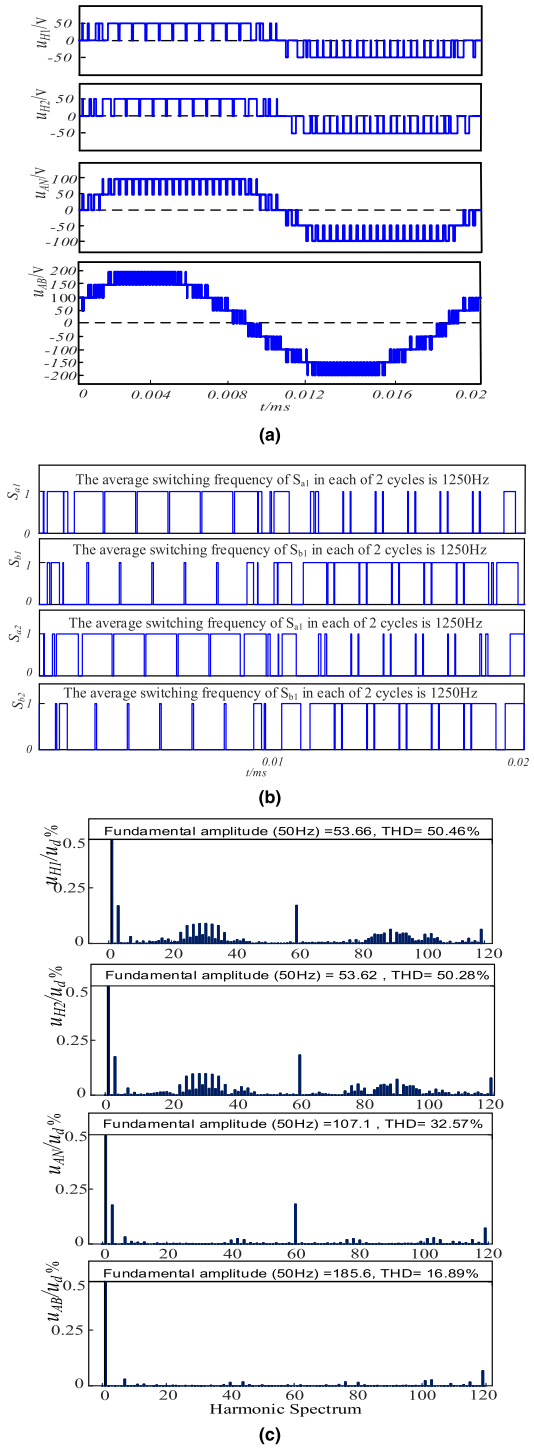

FIGURE 17. Power-balance-based IPD-TPWM modulation strategy (a) Output voltage characteristics of power-balance-based IPD-TPWM strategy (b) Driving signal of the switching tube (c) Harmonic spectrum analysis of output voltage.

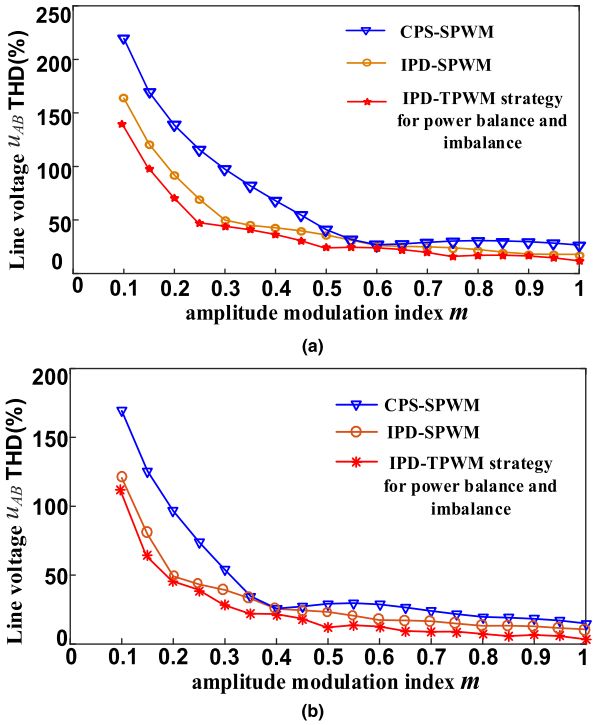

FIGURE 18. Relation curves between output line voltage THD and modulation degree of four modulation strategies (a) Application of CHB Five-level Inverter (b) Application of CHB Seven-Level Inverter.

respectively. IPD-TPWM improves the DC side supply voltage utilization by 19.1% over IPD-SPWM.

Fig.17 show the output voltage waveform, driving signal of the switching tube and harmonic spectrum analysis of the CHB inverter under the power-balance-based IPD-TPWM strategy when the triangulation rate is 0.4 and the modulation ratio is 0.9.

As can be seen from Fig. 17 (a), the on-time of the switch tubes of each cascaded units is the same, and the number of switches is nearly the same, so the output voltage amplitudes are almost equal. As can be seen from Fig. 17 (b), the average switching frequency of all switches is the same in one cycle under this modulation strategy, so the switching losses of the inverters are exactly the same. As can be seen from Fig. 17 (c), the voltage fundamental amplitude and THD value output by u_{H1} and u_{H2} are identical. At the same time, power-balance-based IPD-TPWM retains the advantages of low THD of output voltage and high utilization of DC-side voltage under IPD-TPWM.

Fig. 18 shows the relationship between output line voltage THD and modulation degree under four modulation strategies. When four control strategies are applied to CHB five-level Inverters, the power-balance-based IPD-TPWM strategy and the output THD value under the IPD-TPWM strategy are almost identical throughout the modulation period, and are lower than the THD value of line voltage of IPD-SPWM strategy, effectively improving the quality of the output line voltage, as shown in Fig. 18 (a).

In order to further verify that the power-balance-based IPD-TPWM strategy has not only achieved the lowest THD value of the line voltage under the CHB type five-level inverter, but also can be extended to the N-level CHB inverter. Then four control strategies are applied to the CHB type

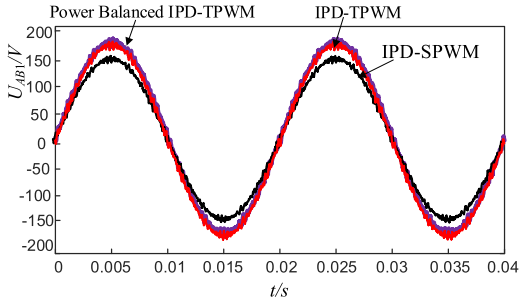

FIGURE 19. Comparison of fundamental voltage amplitude waveforms of three modulation strategies u_{AB}.

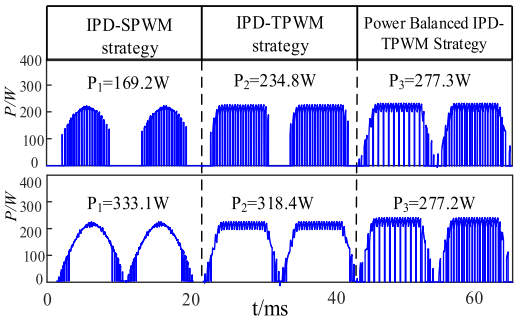

FIGURE 20. Power comparison of three strategies applied to five-level inverters when m = 0.9.

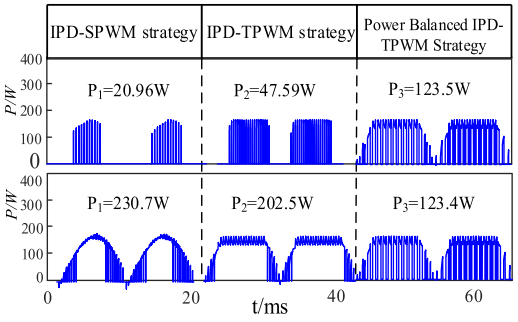

FIGURE 21. Power comparison of three strategies applied to five-level inverters when m = 0.6.

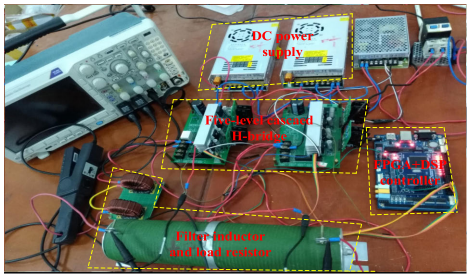

FIGURE 22. Experimental prototype.

seven-level inverter, as shown in Fig. 18(b). The output THD value of power-balance-based IPD-TPWM strategy is the lowest in the whole modulation period, which verifies the practicability and scalability of the proposed power strategy.

Fig.19 shows the comparison of the fundamental amplitudes of three output line voltages u_{AB}. The output fundamental wave voltage amplitude of IPD-SPWM is only 156V, and the DC voltage utilization ratio of IPD-SPWM is the lowest among the three modulation strategies; The output fundamental wave voltage amplitude of IPD-TPWM is 185.6V, which is 19.1% higher than that of traditional IPD-SPWM strategy. It breaks through the limitation that the theoretical maximum voltage utilization can only be increased by 15% when the third harmonic is injected into sinusoidal modulation wave in the Literature [19]. The power-balanced IPD-TPWM retains the advantage of IPD-TPWM increasing DC utilization by 19.1%.

According to Literature [20], when the ratio of fundamental component amplitude of output voltage at AC side of the cascading unit is equal to the ratio of supply voltage at DC side, the discharge characteristics of the cascading unit can be ensured to be consistent, and the power-balance control among the cascading units can be realized. It can be seen from Fig. 17 that the amplitudes of the voltage fundamentals output by the two units H1 and H2 are the same, and the amplitude ratio of the fundamental voltage of the output voltage is 1:1. Therefore, it is considered that H1 and H2 have achieved the effect of power-balance in one switching cycle.

Fig. 20 and Fig. 21 are the power comparison of three control strategies applied to the CHB five-level inverters respectively. It can be seen clearly that IPD-SPWM and IPD-TPWM can not achieve the power-balance of cascaded H-bridges, while power-balance-based IPD-TPWM strategy achieves the power-balance of cascaded H-bridge.

Table 2 shows the comparison of different strategies. It can be seen that the proposed power-balance-based IPD-TPWM strategy has advantages over those proposed in Literature [12]–[16]. This strategy improves the utilization ratio of DC voltage and achieves power-balance in one cycle, and the THD value of output line voltage is the lowest, which effectively improves the quality waveform of output line voltage.

VI. EXPERIMENTAL VERIFICATION

In order to further verify the effectiveness of the proposed control method, a two-unit CHB inverter experimental platform was constructed as shown in Fig.22. The experimental platform is controlled by FPGA +DSP with TX-KP101 as the drive. IGBT IXGH12N60BD1 is selected as the switching tube. The main parameters are as follows: DC input voltage is 50V, output voltage frequency 50Hz, carrier frequency 3kHz, reconstructed carrier frequency = 750Hz, filter inductance L = 2mH, load resistance R = 10 Ω, carrier ratio m_f = 60.

Fig. 23 and 27 show the experimental waveforms of output voltage u_{H1}, u_{H2}, output current i_o and output voltage u_{AN} of the inverters when the modulation degrees are 0.9 and 0.6 respectively under the IPD-TPWM strategy. As can be seen from Fig. 23 (a) and 27 (a), the output voltage waveforms of each cascade unit are obviously different, so the output voltage amplitudes of each unit are quite different.

TABLE 2. Comparison of different strategies.

	DC Side Voltage Utilization	Power-Balance Cycle	Switching Losses Distributed	The Line Voltage v_{AB} THD (%)
PD-TPWM strategy for power-balance	Higher	1 cycle	Balanced	Lower than IPD-PWM
Literature [12]	Higher	/	Unbalanced	Higher than CPS-PWM
Literature [13]	Normal	1 cycle	/	/
Literature [14]	Normal	2 cycle	Unbalanced	Same as IPD-PWM
Literature [15]	Normal	1 cycle	Unbalanced	Same as IPD-PWM
Literature [16]	Normal	1 cycle	Balanced	Higher than or equal to CPS-PWM

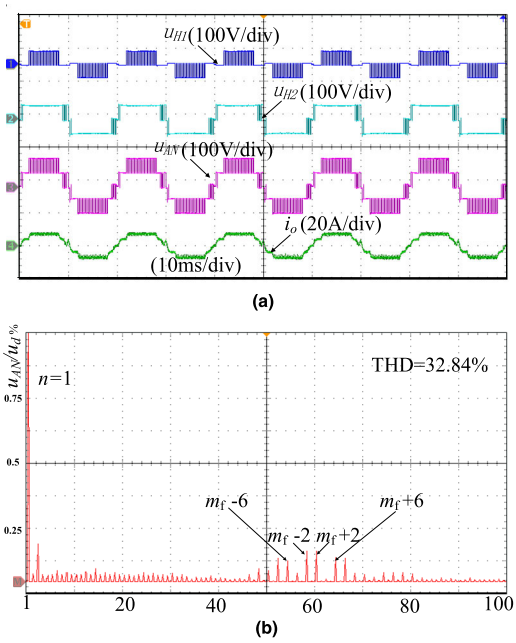

FIGURE 23. IPD-TPWM experiment results (m = 0.9) (a) Output voltage waveform (b) Phase voltage spectrum distribution.

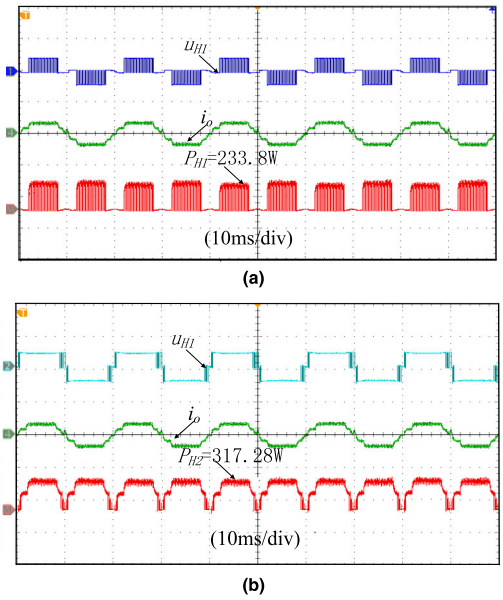

FIGURE 24. Analysis of output power of IPD-TPWM cascade units (m = 0.9) (a) H1-bridge unit (b) H2-bridge unit.

Fig. 23 (b) and 27 (b) are spectrograms of the output voltage u_{AN}. The spectrum of the phase voltage of the strategy is mainly distributed around 3000 Hz, which is almost identical to the spectrum of the output phase voltage in the simulation experiment, further verifying the effectiveness of the proposed IPD-TPWM strategy. Fig. 24 and 28 intuitively show the power comparison of the modulation strategy when the modulation degree is 0.9 and 0.6. The experimental results show that although IPD-TPWM has solved the problem of low utilization of DC voltage, it fails to achieve power-balance of cascade units.

Fig. 25 and 29 show the experimental waveforms of output voltage u_{H1}, u_{H2}, output current i_o and output voltage u_{AN} of the inverters when the modulation degrees are 0.9 and 0.6 respectively under the IPD-TPWM strategy based on power-balance. As can be seen from Fig. 25 (a) and 29 (a), the output voltage waveforms of each cascade unit are basically the same, so the output voltage amplitudes of each unit are almost the same. Fig. 25 (b) and 29 (b) are spectrograms

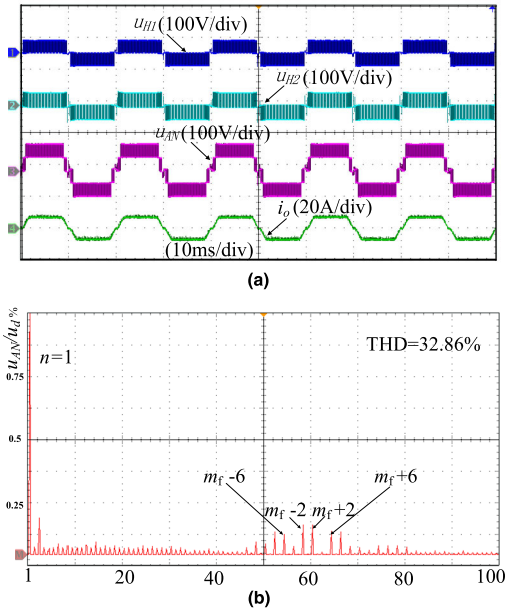

FIGURE 25. IPD-TPWM strategy experimental results in power equalization (m = 0.9) (a) Output voltage waveform (b) Phase voltage spectrum distribution.

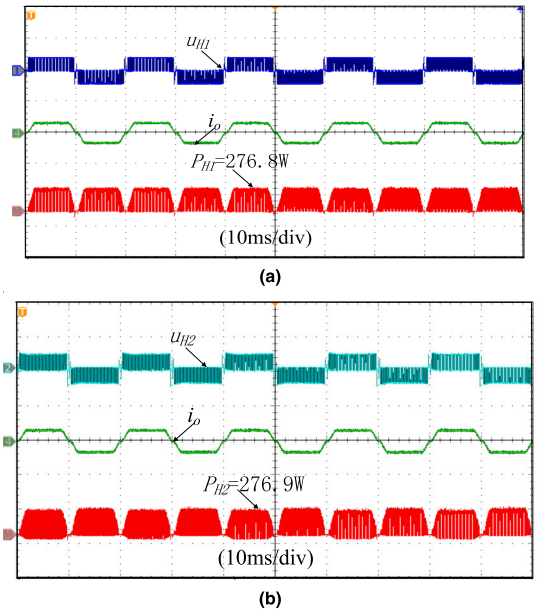

FIGURE 26. Analysis of output power of each unit under IPD-TPWM during power equalization (m = 0.9) (a) H1-bridge unit (b) H2-bridge unit.

of the output voltage u_{AN}. The spectrum of the phase voltage of the strategy is mainly distributed around 3000 Hz, which is almost identical to the spectrum of the output phase voltage under IPD-TPWM strategy..

Fig. 26 and 30 intuitively show the power comparison of the modulation strategy when the modulation degree is 0.9 and 0.6. The experimental results show that when power-balance IPD-TPWM is used, the problem of low utilization rate of DC-side voltage and power-balance is effectively

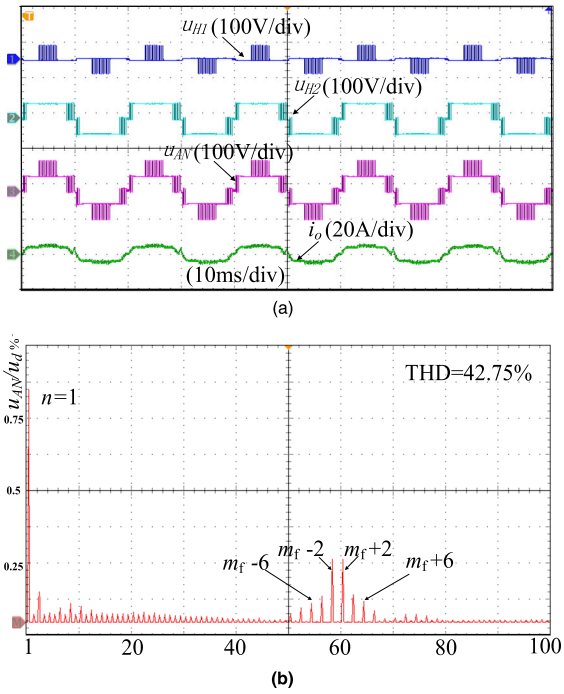

FIGURE 27. IPD-TPWM experiment results (m = 0.6) (a) Output voltage waveform (b) Phase voltage spectrum distribution.

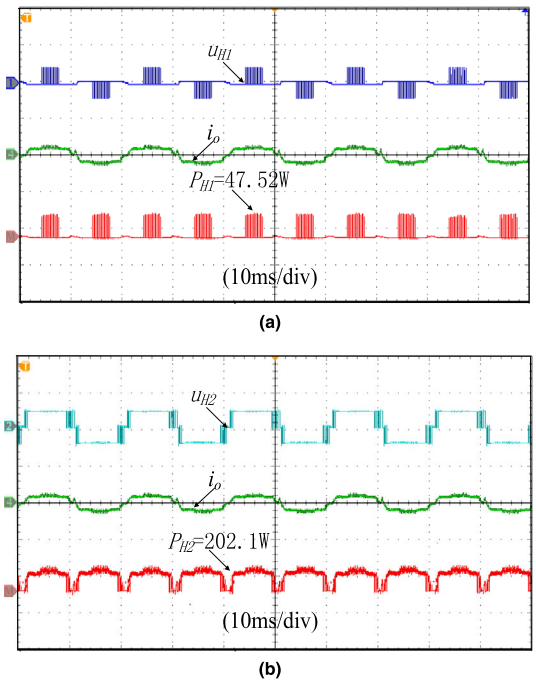

FIGURE 28. Analysis of output power of IPD-TPWM cascade units when power is unbalanced (m = 0.6) (a) H1-bridge unit (b) H2-bridge unit.

solved. At the same time, it can be seen from the experimental phase voltage spectrum distribution that the THD value of this strategy is almost the same as that of traditional IPD-SPWM. The experimental waveforms of IPD-TPWM in power-balance and power imbalance are basically consistent

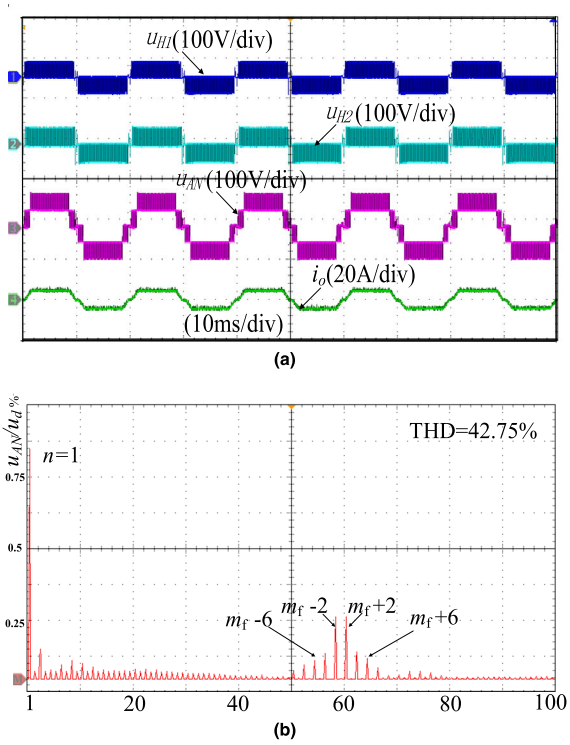

FIGURE 29. IPD-TPWM experimental results in power equalization (m = 0.6) (a) Output voltage waveform (b) Phase voltage spectrum distribution.

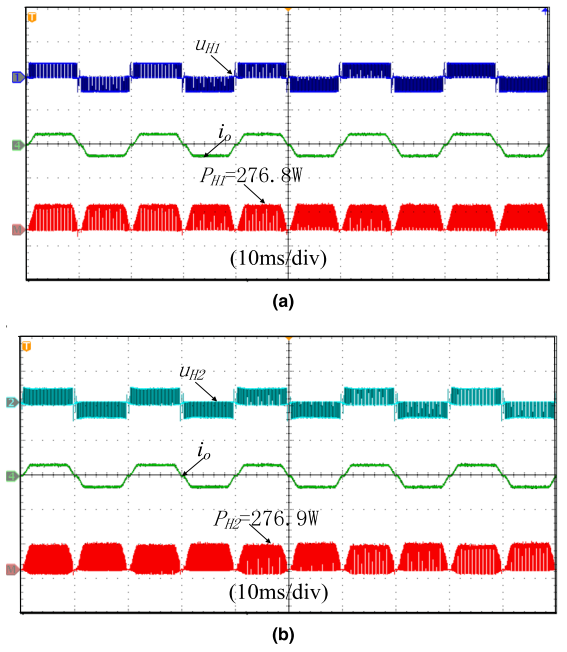

FIGURE 30. Analysis of output power of IPD-TPWM cascade units during power equalization (m = 0.6) (a) H1-bridge unit (b) H2-bridge unit.

with the simulation waveforms, which proves the validity and authenticity of the modulation strategy, and the power-balance control method is relatively simple, and has simplified the control difficulty.

VII. CONCLUSION

Based on the analysis of CHB multilevel inverter, this paper has proposed an power-balance-based in-phase disposition trapezoidal pulse width modulation (IPD-TPWM) strategy, theoretically analyzed the relationship among the amplitude of the output voltage fundamental wave, the trapezoidal wave triangulation rate δ and the output active power, and carried out simulation and experimental verification, which have led to the following conclusions.

(1) For IPD-TPWM, the trapezoidal wave triangulation rate $\delta = 0.4$ is the best trapezoidal modulation wave. IPD-TPWM can make CHB multi-level inverter greatly improve the DC voltage utilization rate to 19.1% without affecting the output phase voltage waveform quality, breaking through the limitation that the third harmonic injection method can only increase the utilization ratio of DC voltage by 15%.

(2) Under the condition of selecting the best trapezoidal modulation wave, the power-balance IPD-TPWM utilizes the switching function state of the inverter redundancy, and by cyclically adjusting the vertical movement of carrier in IPD-TPWM, so that the output voltage amplitude of each cascade unit is the same. Therefore, this strategy has achieved power-balance control over the full modulation ratio range while preserving the advantage that the IPD-TPWM fundamental amplitude has been increased by 19.1%.

(3) Under the power-balanced IPD-TPWM control, the THD value of the CHB inverter output line voltage is lower than that of the IPD-SPWM, and the waveform performance is better. At the same time, the modulation strategy can be extended to the N-level CHB inverter topology. Moreover, the working stress of all the unit switching tubes is the same, the heat dissipation distribution is uniform, the switching loss has been effectively reduced, and the service life and system reliability has been improved.

REFERENCES

[1] L. Zhang, K. Sun, Y. Xing, and J. Zhao, "A family of five-level dual-buck full-bridge inverters for grid-tied applications," *IEEE Trans. Power Electron.*, vol. 31, no. 10, pp. 7029–7042, Oct. 2016.

[2] V. Jammala, S. Yellasiri, and A. K. Panda, "Development of a new hybrid multilevel inverter using modified carrier SPWM switching strategy," *IEEE Trans. Power Electron.*, vol. 33, no. 10, pp. 8192–8197, Oct. 2018.

[3] M. Ye, L. Kang, Y. Xiao, P. Song, and S. Li, "Modified hybrid modulation strategy with power balance control for H-bridge hybrid cascaded seven-level inverter," *IET Power Electron.*, vol. 11, no. 6, pp. 1046–1054, Mar. 2018.

[4] X. Liang and J. He, "Load model for medium voltage cascaded H-bridge multi-level inverter drive systems," *IEEE Power Energy Technol. Syst. J.*, vol. 3, no. 1, pp. 13–23, Mar. 2016.

[5] M. Ye, L. Chen, L. Kang, S. Li, J. Zhang, and H. Wu, "Hybrid multi-carrier PWM technique based on carrier reconstruction for cascaded H-bridge inverter," *IEEE Access*, vol. 7, pp. 53152–53162, 2019.

[6] Y. Li, Y. Wang, and B. Q. Li, "Generalized theory of phase-shifted carrier PWM for cascaded H-bridge converters and modular multilevel converters," *IEEE J. Emerg. Sel. Topics Power Electron.*, vol. 4, no. 2, pp. 589–605, Jun. 2016.

[7] G. Carrara, S. Gardella, M. Marchesoni, R. Salutari, and G. Sciutto, "A new multilevel PWM method: A theoretical analysis," *IEEE Trans. Power Electron.*, vol. 7, no. 3, pp. 497–505, Jul. 1992.

[8] L. Q. Wang and F. Qi, "Novel carrier phase-shifted SPWM for cascade multilevel converter," *Proc. CSEE*, vol. 30, no. 3, pp. 28–34, Mar. 2010.

[9] L. A. Tolbert, F. Z. Peng, T. Cunnyngham, and J. N. Chiasson, "Charge balance control schemes for cascade multilevel converter in hybrid electric vehicles," *IEEE Trans. Ind. Electron.*, vol. 49, no. 5, pp. 1058–1064, Oct. 2002.
[10] J. Liu, Y. Sun, Y. Li, and C. Fu, "Theoretical harmonic analysis of cascaded H-bridge inverter under hybrid pulse width multilevel modulation," *IET Power Electron.*, vol. 9, no. 14, pp. 2714–2722, Aug. 2016.
[11] B. P. McGrath and D. G. Holmes, "Multicarrier PWM strategies for multilevel inverters," *IEEE Trans. Ind. Electron.*, vol. 49, no. 4, pp. 858–867, Aug. 2002.
[12] S. M. Ayob, Z. Salam, and A. Jusoh, "Trapezoidal PWM scheme for cascaded multilevel inverter," in *Proc. IEEE Int. Power Energy Conf.*, Nov. 2006, pp. 368–372.
[13] B. Ge, F. Z. Peng, T. Aníbal de Almeida, and H. Abu-Rub, "An effective control technique for medium-voltage high-power induction motor fed by cascaded neutral-point-clamped inverter," *IEEE Trans Ind. Electron.*, vol. 57, no. 8, pp. 2659–2668, Aug. 2010.
[14] D. Sreenivasarao, P. Agarwal, and B. Das, "Performance evaluation of carrier rotation strategy in level-shifted pulse-width modulation technique," *IET Power Electron.*, vol. 7, no. 3, pp. 667–680, Mar. 2014.
[15] M. Angulo, P. Lezana, and S. Kouro, "Level-shifted PWM for cascaded multilevel inverters with even power distribution," in *Proc. IEEE Power Electron. Spec. Conf. (PESC)*, Orlando, FL, USA, Jun. 2007, pp. 2373–2378.
[16] I. Sarkar and B. G. Fernandes, "Modified hybrid multi-carrier PWM technique for cascaded H-bridge multilevel inverter," in *Proc. 40th Annu. Conf. IEEE Ind. Electron. Soc.*, Oct./Nov. 2014, pp. 4318–4324.
[17] F. Zhang and X. Qian, "Improved GK clustering algorithm," *J. Comput. Appl.*, vol. 32, no. 9, pp. 2476–2479, 2012.
[18] X. Wang, X. Zhang, and X. Ruan, "Optimal SPWM control strategy and its power balance scheme for cascaded multilevel inverters," *Trans. China Electrotech. Soc.*, vol. 24, no. 5, pp. 92–99, 2009.
[19] E. Guan, P. Song, and M. Ye, "Three-phase inverter with four bridge legs based on three harmonic injection method," *Trans. China Electrotech. Soc.*, vol. 20, no. 12, pp. 43–46, 2005.
[20] Y. Sun and X. Ruan, "Power balance control schemes for cascaded multilevel inverters," *Proc. CSEE*, vol. 26, no. 4, pp. 126–133, 2006.

MANYUAN YE received the B.Eng. degree in industrial automation from the Anhui University of Science and Technology, Huainan, China, in 2001, and the M.Sc. degree in traffic control and information engineering from East China Jiaotong University (ECJTU), Nanchang, China, in 2004, where he is currently pursuing the Ph.D. degree.

He is an Associate Professor with the School of Electrical and Automation Engineering, ECJTU. His research interests include power electronics and electric drives, modular multilevel converter, pulse width modulation, and selective harmonic elimination techniques.

WEI REN received the B.Eng. degree in information and computing science from the Inner Mongolia University of Science and Technology, Baotou, China, in 2018. He is currently pursuing the M.Sc. degree with ECJTU, Nanchang, China. His research interests include power electronics and cascaded multilevel converter.

LE CHEN received the B.Eng. degree in electrical engineering from the Shaanxi University of Science and Technology, Xi'an, China, in 2016. He is currently pursuing the M.Sc. degree with ECJTU, Nanchang, China. His research interests include power electronics and cascaded multilevel converter.

QIWEN WEI received the B.Eng. degree in electrical engineering from East China Jiaotong University, Nanchang, China, in 2018, where he is currently pursuing the M.Sc. degree. His research interests include power electronics and cascaded multilevel converter.

GUIZHI SONG received the B.Eng. degree in electrical engineering from East China Jiaotong University, Nanchang, China, in 2018, where he is currently pursuing the M.Sc. degree. His research interests include power electronics and cascaded multilevel converter.

SONG LI received the M.Sc. degree in traffic control and information engineering from East China Jiaotong University (ECJTU), Nanchang, China, in 2005. She is currently an Associate Professor with the School of Electrical and Automation Engineering, ECJTU. Her research interests include power electronics.